

Cite this: *Energy Environ. Sci.*, 2011, **4**, 3263

www.rsc.org/ees

## PERSPECTIVE

### Wiring photosynthetic enzymes to electrodes†

Adrian Badura,<sup>a</sup> Tim Kothe,<sup>a</sup> Wolfgang Schuhmann<sup>b</sup> and Matthias Rögner<sup>\*a</sup>

Received 11th March 2011, Accepted 10th June 2011

DOI: 10.1039/c1ee01285a

The efficient electron transfer between redox enzymes and electrode surfaces can be obtained by wiring redox enzymes using, for instance, polymer-bound redox relays as has been demonstrated as a basis for the design of amperometric biosensors, logic gates or sensor arrays and more general as a central aspect of “bioelectrochemistry”. Related devices allow exploiting the unique catalytic properties of enzymes, among which photosynthetic enzymes are especially attractive due to the possibility to trigger the redox reactions upon irradiation with light. Photocatalytic properties such as the light-driven water splitting by photosystem 2 make them unique candidates for the development of semiartificial devices which convert light energy into stable chemical products, like hydrogen. This review summarizes recent concepts for the integration of photosystem 1 and photosystem 2 into bioelectrochemical devices with special focus on strategies for the design of electron transfer pathways between redox enzymes and conductive supports.

#### Introduction

Among all energy converting processes on earth—including non-biological—oxygenic photosynthesis is by far the most important. Notably, this process requires only water and sunlight as energy sources; their combination enables CO<sub>2</sub> fixation which finally provides us with food and biomass.

Oxygenic photosynthesis is also the historic source of our fossil fuels that drive our technologies while having a serious impact on

our environment and climate. Besides the challenge to decode the basic molecular mechanism which efficiently converts solar energy into chemical energy, photosynthesis could also be considered a marvellous source of inspiration for the development of techniques which will help to harness solar energy for our future energy demands beyond fossil fuels.

The arrangement of chlorophylls as antennae within the matrix of photosynthetic proteins allows an efficient capture of light and the transfer of its energy to the reaction centres, where charge separation occurs. In turn, the arrangement of cofactors optimizes the transfer of electrons from the inner reaction centre to the protein periphery connected with a decrease of the formal potentials of the cofactors, where finally the energy is stored in a stable compound. Starting from the oxidation of water at photosystem 2 (PS2) to the reduction of ferredoxin by photosystem 1 (PS1) the electron overcomes a remarkable potential difference of about 1.5 eV.<sup>1–3</sup>

As the photosynthetic efficiency decreases with the number of downstream processes, each living cell finally uses more than

<sup>a</sup>Plant Biochemistry (Faculty of Biology & Biotechnology), Ruhr-University Bochum, Universitätsstrasse 150, D-44780 Bochum, Germany. E-mail: matthias.roegner@rub.de; Fax: +49 2343214322; Tel: +49 2343223634

<sup>b</sup>Analytische Chemie – Elektroanalytik & Sensorik, Ruhr-University Bochum, Universitätsstrasse 150, D-44780 Bochum, Germany

† This article was submitted as part of a Themed Issue on biomimetic approaches to artificial photosynthesis. Other papers on this topic can be found in issue 7 of vol. 4 (2011). This issue can be found from the EES homepage [http://www.rsc.org/ees].

#### Broader context

Solar energy is by far the most important renewable energy source on our planet. It is harnessed most efficiently by photosynthesis, the primary process which is the basis for continuous synthesis of life on earth, but also a blue print for conversion and storage of energy originating from sunlight and water. The early events of this reaction—especially the light-induced charge separation within the photosynthetic enzymes—occur with an unsurpassed efficiency. As the complexity of subsequent reactions in biological cells leads to a considerable decrease of this efficiency, profitable use of this process requires that the captured light energy is harnessed at the earliest stage possible. This can be realized by the integration of isolated photosynthetic complexes into bioelectrochemical devices for which the electric coupling to conductive supports/electrodes by “molecular wires” turned out to be the most relevant step. Optimized “wiring” enables (a) the exploring of the capacity and the limits of these light-triggered reactions irrespective of cellular restrictions and (b) the estimation of their potential for technical applications in bio-inspired artificial systems for solar energy conversion or biosensing.

95% of the incident light energy for metabolic processes, with less than 5% remaining as energy stored in form of biomass.<sup>4</sup> For this reason, it seems to be attractive to harvest the power of light energy as early as possible in the reaction chain of events. Photosynthetic reaction centers (RC) are designed to use a fraction of the captured light energy for increasing the distance between light-induced electron hole pairs by allowing an extremely fast redox reaction to occur from the excited state of the chlorophyll to a primary electron acceptor. This leads to an increased lifetime of the electron hole pair and enables diffusion controlled follow up redox reactions with soluble partners. For this reason the integration of photosynthetic RCs into bioelectrochemical devices can provide knowledge on parameters which limit the catalytic properties of isolated photosynthetic enzymes and on the potential to maximise the harvesting of electrons from these systems.<sup>5</sup>

The basis for an integration of photosynthetic RCs into semi-artificial systems is the establishment of efficient and reproducible isolation procedures for the membrane proteins PS1 and PS2 (see, e.g. ref. 6 and 7), and the knowledge of their 3D-structures at high resolution, which yield a profound insight into structure/function principles.<sup>8–11</sup> The information on the molecular level provides an excellent blue print for the introduction of photosynthetic RCs into bioelectrochemical and semi-artificial energy converting devices. Photosynthetic RCs are also in the focus of other technological applications such as biosensors for environmental screenings or opto electronic devices as optical memories or amplifiers.

The integration of redox enzymes into bioelectrochemical devices requires immobilisation procedures which generate a spatially organised biointerface on a conductive support. Immobilisation comprises the attachment of enzymes *via* electrostatic interactions, affinity interactions, covalent binding or entrapment within (redox/conducting) polymers on various conductive and semiconductive supports (for detailed reviews see ref. 12 and 13). According to Marcus theory of electron transfer the rate of the electron exchange between enzyme and conductive support is—besides the potential difference and the reorganisation energy—mainly governed by the distance between the electron donor and acceptor.<sup>14</sup> As the active sites are often buried deeply within the protein shell, the electron transfer rate is significantly decreased. Thus, electron transfer (ET) pathways between the active site of the immobilized enzyme and the conductive support have to be designed for an efficient electron transfer communication. While many methods for this so-called “wiring of enzymes” are available, the most simple consists of free diffusing native or artificial redox mediators, which are oxidized or reduced at the conductive support, diffused into the active center of the redox protein where they accept or donate electrons before they diffuse back to the electrode surface. The activity of the enzyme can then be monitored *via* a current response. More elaborate methods comprise the chemical modification of enzymes with redox relay units, the extraction of cofactors followed by reconstitution of the apo-enzyme with surface bound redox mediators and the entrapment of the enzymes within three-dimensional networks of redox/conducting polymers.

This review focuses on methods for the integration of PS1 and PS2 into bioelectrochemical devices mainly aiming at providing an overview on strategies for the design of electron transfer

pathways which are vital for the efficient communication of immobilized enzymes with conductive supports. Progress in this field could provide a major contribution towards coupling of light-triggered photosynthetic processes with biofuel production such as the formation of molecular hydrogen from water.

## What comprises “wiring”?

In this review “wiring” comprises the immobilisation of the photosynthetic RCs on conductive support materials including the establishment of efficient ET pathways for the purpose of photocurrent generation. These electrochemical measurements are an important indicator for the functional ET to, from and through these photosynthetic RCs and can provide essential information about the maximum possible ET rate under optimal conditions and without compromising with the limitations imposed by living cells. Photocurrent measurements and especially photocurrent voltammetry can provide important information about rate-limiting steps.

## Photosystem 2 in bioelectrochemical devices

Photosystem 2 (PS2) represents a multi-subunit cofactor enzyme which is embedded in the thylakoid membrane of higher plants, green algae and cyanobacteria and catalyses light-driven water splitting. Water splitting combined with the light induced reduction of ferredoxin by photosystem 1 (PS1) supplies protons and electrons which finally enable biomass formation. The light-triggered reaction of PS2, which was recently revised (see ref. 15) starts with the absorption of a photon which either directly or *via* excited state energy transfer from the antenna chlorophyll leads to charge separation within the reaction center.<sup>16,17</sup> In a sequence of ET reactions (see Fig. 1a, b), starting with the primary donor of the charge separated state,  $\text{Chl}_{\text{D1}}$ , and proceeding *via* pheophytin to quinone A, the first stable radical pair  $\text{P}_{\text{D1}}^+\text{PheoQ}_\text{A}^-$  is formed.<sup>18,19</sup>  $\text{P}_{\text{D1}}^+$  in turn drives the oxidative water splitting at the  $\text{Mn}_4\text{O}_5\text{Ca}$  complex,<sup>15</sup> with a redox active tyrosine  $\text{Tyr}_\text{Z}$  mediating the stepwise extraction of four electrons from the water-oxidizing complex (WOC). At the so-called acceptor site of PS2,  $\text{Q}_\text{A}^-$  induces the reduction of plastoquinone-9<sup>20</sup> in two successive one electron reactions to  $\text{PQH}_2$ , the enzymatic product that is released from PS2. This reaction occurs in a binding pocket called  $\text{Q}_\text{B}$ -site which provides direct access to the enzyme for a number of artificial electron acceptors: suitable electron acceptors are usually benzoquinone-derivates like 1,4-dichlorobenzoquinone or substituted indamines.<sup>21,22</sup> These acceptors are commonly used as sacrificial reagents to determine the light induced  $\text{O}_2$  evolution rates of isolated PS2 complexes or of membrane fractions with missing natural acceptor. On the other hand the  $\text{Q}_\text{B}$ -pocket is also the binding site for numerous herbicides which block the ET sequence.<sup>23</sup>

For the integration of PS2 into bioelectrochemical devices we can in a first attempt ignore the complex reactions within the photosynthetic RC and treat it as an ordinary redox enzyme. Moreover, one has just to consider the acceptor site, as the donor site receives electrons directly from the water splitting process at the WOC. Decisive parameters comprise a) an immobilisation strategy, which should preserve the activity of PS2 on the electrode surface, b) two “substrates”: light and water, and c) a redox

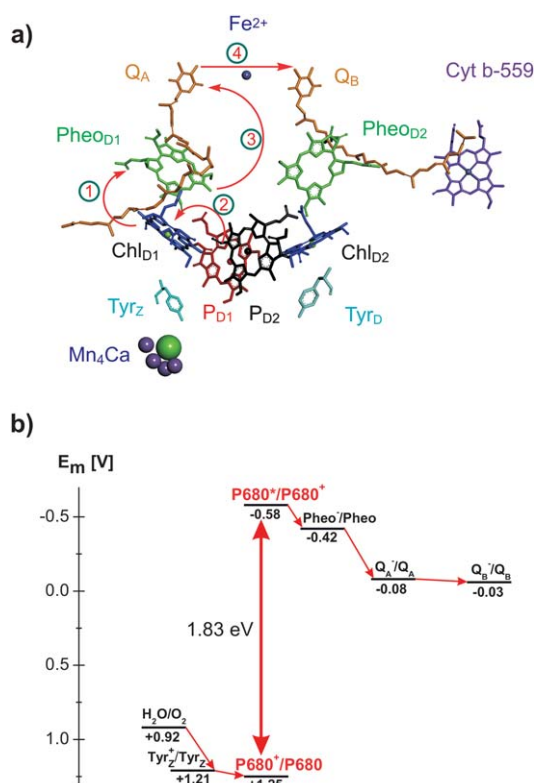


**Fig. 1** a) Cofactor arrangement of the ET chain of PS2 showing the ET pathway (arrows). The order of the reaction sequence is highlighted by encircled numbers. b) Redox potential scheme of the cofactors involved in the ET reaction sequence of PS2 in accordance with the revised reaction sequence (P680 represents P<sub>D1</sub>, P<sub>D2</sub>, Chl<sub>D1</sub>, Chl<sub>D2</sub>) (according to ref. 2).

mediator with suitable redox potential ( $> -0.03$  V vs. NHE, see Fig. 1b) and affinity to the Q<sub>B</sub>-site of PS2, which also has to be reduced or oxidized at a suitable potential at the electrode surface.

The basic concept is schematically depicted in Fig. 2. Upon excitation of immobilised PS2 with light, water splitting provides electrons for the reduction of a redox mediator, which in turn is oxidized at an electrode surface, if a suitable potential is applied.

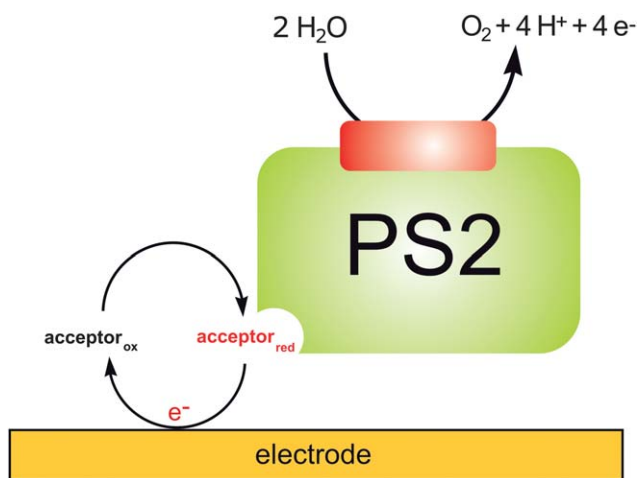


**Fig. 2** Basic principle for the integration of PS2 into bioelectrochemical devices (for details see text).

The determined photocurrent under potentiostatic control is proportional to the immobilized PS2 activity.

A first application of immobilized PS2 was demonstrated in an amperometric biosensor for the detection of herbicides in water. Koblizek *et al.*<sup>24</sup> reported the entrapment of PS2 particles, which had been isolated from the thermophilic cyanobacterium *Thermosynechococcus elongatus*, within gelatine, agarose and a bovine serum albumin<sup>25</sup> matrix mixed with glutaraldehyde. PVC sheets modified with a graphite ink were used as electrodes, and duroquinone and ferricyanide served as freely diffusing redox mediators. Although this system suffered from low current signals, the inhibition by classical herbicides like atrazine or DCMU indicated its function as simple biosensor.

In addition, several studies reviewed by M. Giardi and E. Pace showed the ability of isolated PS2 complexes and PS2 enriched membrane fragments to act as amperometric biosensors which are sensitive towards different classes of herbicides and heavy metals.<sup>26</sup>

Maly *et al.*<sup>25</sup> immobilised PS2 onto thiolated gold electrodes which had been modified by terminal Ni-nitrilotriacetic acid groups (NiNTA). This is a common method for the immobilization of enzymes which were previously modified with a genetically introduced polyhistidine-tag.<sup>27,28</sup> The tag allows a reversible and oriented binding *via* metal affinity interactions to the exposed NTA-functionality on the gold surface. Due to the further introduction of BSA as a “spacer” molecule within the immobilized PS2 layer the electrode response was increased to  $0.055 \mu\text{A cm}^{-2} \text{mW}^{-1}$ . This was attributed to an optimized mass transport of the redox mediator to the immobilised PS2 molecules. However, the discrepancy between calculated current densities—based on the amount of immobilized PS2 complexes—and the measured current density, was in the range of four orders of magnitude. This may be due to various parameters such as the activity of the immobilised enzyme, the choice of the redox mediator and mass transport limitations. To overcome the latter, Maly and co-workers modified gold electrodes by electrodeposition with mercapto-p-benzoquinone under formation of a layer on which unmodified PS2 could adsorb.<sup>29</sup> Current densities of up to  $0.5 \mu\text{A cm}^{-2} \text{mW}^{-1}$ , *i.e.* about a 10-fold increase, showed that this layer can shuttle electrons between PS2 (Q<sub>A</sub>-site) and the electrode surface. In contrast to the initial approach using His-tagged PS2, the adsorbed PS2 particles are randomly orientated on the electrode surface. Thus, only PS2 particles which are facing the benzoquinone layer with their Q<sub>A</sub>-site are connected for successful ET. This is additionally related to the fact that the formed polymer chains are too short—about 6 nm—as compared with the dimensions of the PS2 molecule ( $20.5 \times 11 \times 4.5 \text{ nm}$ )<sup>2,8</sup> to reach the acceptor site of each adsorbed PS2.

In 2006 we developed a system with considerably higher current densities, using immobilized PS2 from the same organism.<sup>30</sup> His-tagged PS2 was specifically bound *via* metal affinity interactions on a self-assembled monolayer of long chains (C<sub>16</sub>) of carboxyalkylthiolates modified with NiNTA-groups. Unspecific protein binding onto the electrode surface was prevented by an excess of the shorter 1-octanethiol which controlled the amount of NiNTA-groups during the generation of the SAM (Fig. 3). According to surface plasmon resonance

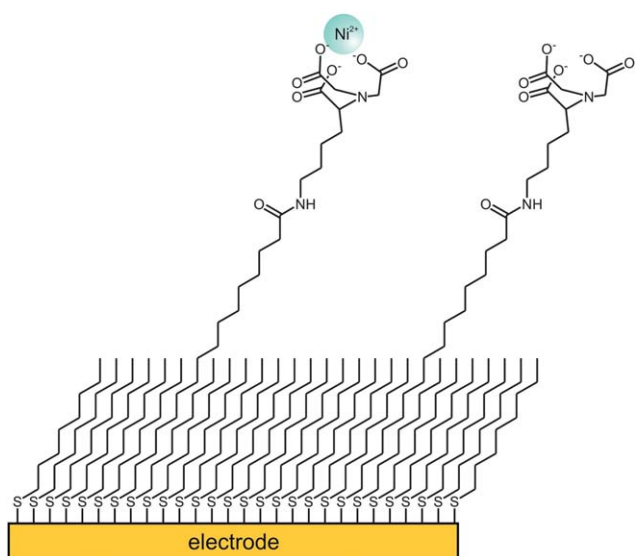


**Fig. 3** Scheme for structuring a gold surface with mixed thiolates (1-octanethiol and 16-mercaptoethanoic acid). Carboxy groups were activated with NHS/EDC for binding of Amino-NTA, which forms a complex with  $\text{Ni}^{2+}$  ions. (Reproduced from ref. 30).

measurements, a layer with  $\sim 80\%$  specifically bound PS2 molecules was generated on the gold surface. This limited amount of immobilized PS2 prevented mass transport limitation of the soluble redox mediator 2,6-dichloro-1,4-benzoquinone as compared with an overcrowded protein layer.

A current density of up to  $\sim 8 \mu\text{A cm}^{-2} \text{mW}^{-1}$  was achieved which is equivalent to an  $\text{O}_2$ -evolution rate of  $6400 \mu\text{mol O}_2 \text{mg}^{-1} \text{Chl h}^{-1}$ . This is the highest ever reported activity of isolated PS2 particles<sup>7</sup> and confirms that the activity of immobilized PS2 is preserved under these conditions.

As a matter of fact, the amount of PS2 which can be immobilized within a monolayer on a surface is limited. Theoretical calculations indicate a monolayer coverage of about  $0.4 \text{ pMol cm}^{-2}$ .<sup>30</sup> For this reason, higher current densities can only be expected if the amount of immobilized PS2 can be increased or if the ET rate can be optimized. Both effects can be combined by the use of osmium-complex modified redox polymers which fulfill both the role of a 3-dimensional immobilisation matrix and of a redox mediator. Previously, redox polymers had been successfully applied for the development of reagentless biosensors (*e.g.* glucose sensors).<sup>31–34,45</sup> For PS2, the principle of a “wired” enzyme is schematically shown in Fig. 4. While the polymer immobilizes PS2 by the formation of a cross-linked three-dimensional hydrogel with a mesh width which is smaller than the size of the protein, its hydrogel character still enables small molecules to diffuse into the swollen polymer matrix. The ET is realized by an electron hopping mechanism between neighbouring redox centers consisting of polymer-bound Os complexes which, finally, allows the transfer of electrons from the active centre of PS2 to the electrode surface by means of a sequence of self-exchange ET reactions between neighbouring polymer-bound Os complexes.<sup>12</sup> In our study Os-bis-*N,N*-(2,2′-bipyridyl)-dichloride was attached to a poly-imidazol polymer backbone *via*

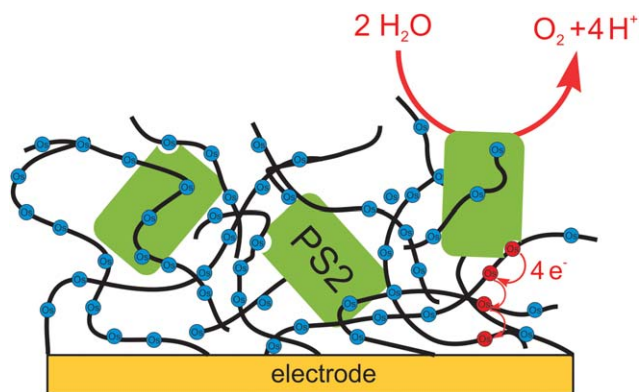


**Fig. 4** PS2 embedded within a polymer matrix which is modified by Os-complexes; red arrows indicate the ET from the  $\text{Q}_\text{B}$ -site to the electrode (according to ref. 35).

a ligand exchange reaction under liberation of one  $\text{Cl}^-$ -ligand and coordinative binding of a polymer-attached imidazolyl moiety.<sup>35</sup> PS2 entrapped within this matrix showed current densities in the range of  $\sim 18 \mu\text{A cm}^{-2} \text{mW}^{-1}$  under illumination. The operational stability was improved about from  $t_{1/2} = 18 \text{ min}$  to about  $t_{1/2} = 245 \text{ min}$  as compared with the previously reported monolayer system.<sup>30</sup> This is most probably due to the fast ET between PS2 and the redox polymer, which reduces the light induced damage of PS2 by reactive oxygen species or the damage of the water oxidizing complex itself.<sup>15,36,37</sup>

The introduction of Os-complex-modified redox polymers provided an extremely simple method for the effective immobilisation of PS2, since the pretreatment is reduced to a drop coating procedure in which isolated PS2 complexes are mixed with a polymer solution and a cross-linker (*e.g.* poly(ethylene glycol)diglycidyl ether) followed by deposition on the electrode surface. The synthesis of tailored redox polymers with predefined properties and redox potentials may lead to further improvements: in combination with non-manual deposition methods, catalytic interfaces with increased reproducibility and stability can be generated.<sup>38</sup>

In summary, these PS2 coated electrodes represent an interface for the heterogeneous catalysis of water oxidation. Under illumination, they are capable of water splitting at oxidation potentials as low as  $\sim 0 \text{ V vs. NHE}$ .<sup>35</sup> In contrast, other artificial devices for water oxidation require overpotentials in the range of  $\sim 1.3 \text{ V}$ ,<sup>39</sup> which emphasizes the outstanding performance of PS2. At  $>20\%$ , the overall solar conversion efficiency of PS2 is in the range of good silicon solar cells. The latter, however, are lacking the ability for catalytic water oxidation.<sup>40</sup> On the other hand, PS2 still suffers from a low operational stability when exposed to light. Under physiological conditions in a plant cell, the ongoing function of PS2 is secured by a very efficient repair cycle, which replaces the central D1 subunit of the complex with a high turnover rate including most of the cofactors.<sup>41,42</sup> This repair mechanism, which results in a physiological half-life time for the D1 subunit of 20–30 min cannot be realized in a semi-artificial photochemical cell with immobilized PS2.<sup>43</sup> This is the major reason why such systems are important as proof of principle, but most probably have to be replaced by biomimetic light driven power supplies for larger technological devices in the future.



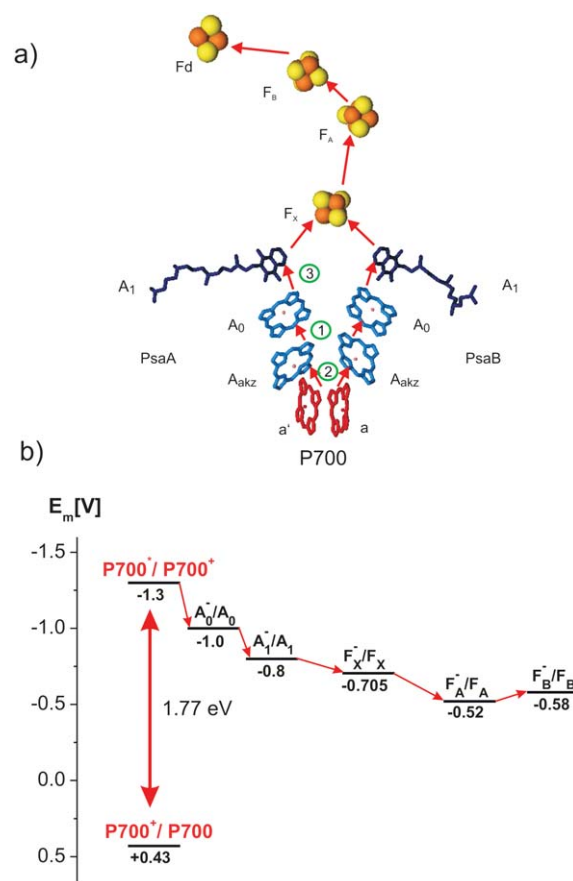
## Wired PS2: Outlook

Table 1 summarizes the photocurrents with immobilized PS2 as achieved with various electron acceptors. The considerable increase in current density by systematic improvements within a rather short period of time indicates the high potential of this bioelectrochemical approach, especially as the immobilization procedures could be highly simplified in parallel. The lifetime of PS2 could be increased considerably which may be due to avoiding the formation of reactive oxygen species by efficient ET processes. The evaluation of the parameters influencing and limiting the ET processes between immobilised PS2 and electrode surfaces can be studied in simple model systems providing interesting hints concerning avoiding/minimising light damage in biomimetic PS2 constructs. For processes within the protein itself, the combination of bioelectrochemical methods with fluorescence spectroscopy or infrared spectroscopy, as already demonstrated for cytochrome oxidase,<sup>27</sup> might lead to a better understanding of ET reactions including their potential and limitations.<sup>44</sup> Especially the use of redox or conducting polymers enables the control of the light-driven reactions simply by modulating precisely the applied potential and thus the activity of the enzyme.

These informations may serve as a benchmark for improving performance and lifetime of PS2 and for the development of artificial model compounds—for instance for an efficient generation of bioenergy using water and sunlight (see last section).

## Integration of PS1 into bioelectrochemical devices

Photosystem 1 (PS1) represents the largest *trans*-membrane multi-subunit protein complex.<sup>6</sup> It catalyzes the translocation of electrons from plastocyanin (or cytochrome  $c_6$ ) on the luminal side to ferredoxin (or flavodoxin) on the cytoplasmic side of the thylakoid membrane. The driving force for this endergonic reaction is supplied by the absorption of visible light by PS1. This leads to the formation of an electronically excited state which is accompanied by a substantial change in the redox potential of the reaction center from +0.43 V to -1.3 V.<sup>46,47</sup> The overall reaction sequence (see Fig. 5a) was recently revised. In accordance with new spectroscopic data the accessory chlorophyll  $A_{acc}$  is now considered to be the primary electron donor which undergoes charge separation due to the absorption of a photon, resulting in the first radical pair  $Chl_{acc}^+ChlA_0^-$ .<sup>48,49</sup> Thereafter P700 (formerly regarded the primary donor) is oxidized. At the acceptor side, a series of cofactors guides the inner protein ET with contribution from both cofactor branches along with a decrease of the potential.<sup>46,47,50</sup> The final light induced redox



**Fig. 5** a) Cofactor arrangement of the ET chain in PS1 (arrows indicate the ET pathway). For a better understanding the first three steps of the reaction sequence are highlighted with encircled numbers. b) Redox potential scheme of the components involved in ET of PS1 in accordance with the revised reaction sequence (P700 implies  $Chl_a$ ,  $Chl_a'$  and  $Chl_{acc}$ ) (according to ref. 1, 46, 47, 55).

potential difference between the donor,  $P700^+$  and the acceptor site,  $F_B^-$ , is about 1 V, representing a thermodynamic efficiency of nearly 60% for a red-light photon. As each absorbed photon generates a charge separated state,  $P700^+/F_B^-$ , the quantum yield approaches almost 1.<sup>1,51</sup>

These outstanding photocatalytic properties make PS1 particularly suitable for the conversion of visible light into chemical energy by means of specifically designed bioelectrochemical devices.<sup>30,52</sup>

Interestingly, the number of PS1-related articles within the field of optoelectronics and bioelectrochemistry by far exceeds

**Table 1** Summary: Photocurrents with PS2<sup>a</sup>

Procedure	Acceptor	Current density ( $\mu A\ cm^{-2}\ mW^{-1}$ )	Ref.
Monolayer on Ni(II)NTA-SAM/BSA spacer	Duroquinone	0.055	25
Adsorbed on electrodeposited layers of the acceptor	Mercapto-p-benzoquinone	0.5	29
Monolayer on Ni(II)NTA-SAM	2,6-Dichloro-1,4-benzoquinone	8	30
Os complex modified polymer matrix	Os complexes	18	35

<sup>a</sup> Current densities were standardised to an irradiation intensity of  $1\ mW\ cm^{-2}$ .

PS2-related articles. This may be due to the higher stability of PS1 in combination with the possibility to manipulate its internal ET pathway without strongly affecting its function. Also, integration of this enzyme into solid state devices<sup>53,54</sup> and various bioelectrochemical systems underlines its unique catalytic activity.

### Direct ET between PS1 and electrode surfaces

The most straightforward ET pathway of immobilised redox protein is the direct electron transfer between the active site of the redox protein and the electrode surface. Typically for large protein complexes, and also in the case of PS1, the active sites are usually embedded in the interior of the protein, so that direct ET is unexpected. As a matter of fact, direct electron transfer is only possible after a proper orientation of the PS1 complex with the active site in the closest possible proximity to the electrode surface. One attempt was seen in the proper orientation of PS1 at self-assembled monolayers (SAM) composed from  $\omega$ -organothiols:

a) Lee *et al.*<sup>56</sup> used  $-OH$ ,  $-COOH$  and  $-SH$  modified SAMs to immobilise PS1 by electrostatic interactions in different orientations on gold surfaces. A preferentially parallel orientation on the  $-COOH$  surface was suggested. A potential scan (current–voltage curve) resulted in a semiconductor-like behaviour with a bandgap of  $\sim 1.8$  eV in accordance with the energy gap between P700 and P700\*. A diode-like behaviour was observed on an  $-OH$  terminated SAM surface with a preferentially perpendicular orientation of PS1, while  $-SH$  modified surfaces showed no preferential orientation of PS1.

b) Munge *et al.*<sup>57</sup> used protein film voltammetry for the electrochemical characterization of immobilized PS1 complexes on pyrolytic edge-plane graphite electrodes. The electrochemical response could be assigned to the cofactors  $A_1$  and  $F_A$  of PS1. Adsorption of PS1 onto gold electrodes modified with hydroxyl-terminated SAMs enabled both the signals of P700 and the  $F_A/F_B$  peaks in one cyclic voltammogram. Weak photocurrents in the range of  $3 \text{ nA cm}^{-2}$  could be observed with methyl viologen as electron acceptor.<sup>58</sup> As electron transfer in PS1 occurs in less than  $1 \mu\text{s}$ , photocurrent densities of about  $1 \text{ mA cm}^{-2}$  can be expected, assuming an immobilised monolayer of PS1 with  $0.5 \text{ pMol cm}^{-2}$  coverage.<sup>1,59</sup> To overcome this discrepancy, an efficient ET pathway between PS1 and the electrode surface has to be designed.

### Wiring of PS1

In PS1 the reduction and oxidation of the redox partners occur on opposite sides of the complex which are additionally separated under physiological conditions by the thylakoid membrane. The ET pathway is sterically predefined to optimise the yield of photogenerated products and maximise energy storage. However, if the protein is not isotropically orientated within a lipid bilayer, both recombination and short circuit of the redox partners and/or PS1 have to be avoided. The basic principle is schematically illustrated in Fig. 6: light excitation of immobilized PS1 results in the reduction of the electron acceptor ( $F_B$ -cluster) and the oxidation of the donor. Electrochemical monitoring of these reactions requires the application of

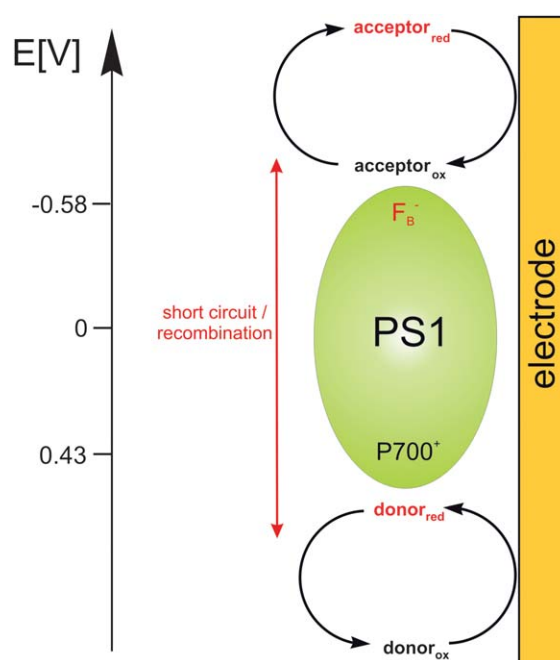


**Fig. 6** Integration of PS1 into bioelectrochemical devices including possible short circuit or recombination pathway between the redox partners.

a potential to the electrode which is adjusted to reduce the oxidized donor species. However, due to the necessary difference in the formal potential of the donor and the acceptor species this electrode potential will be sufficient to oxidize the acceptor and leads by this to a complete loss of any measurable photocurrent (see Fig. 6). For this reason, a PS1-dependent net photocurrent is only detectable if the rate of either the donor reduction or acceptor oxidation at the electrode surface differ at least slightly from each other one, for instance, through a coupled follow-up reaction. For a follow-up reaction at the acceptor site methyl viologen (1,1'-dimethyl-4,4'-bipyridinium) is a good example. It is faster reoxidized by  $O_2$  in the bulk solution than reduced by PS1 or oxidized at the electrode (for details see below).

### Mediated ET between PS1 and electrode surfaces

**a) Freely diffusing redox mediators.** To utilize enzymatic reaction effectively within a bioelectrochemical set-up the activity of the enzyme within the artificial environment is one of the most important parameters, which can be easily quantified by measuring the catalytic current (for a summary see Table 2). Freely diffusing redox mediators offer the easiest way to establish an ET communication between PS1 and a suitable electrode surface. Faulkner *et al.*<sup>60</sup> reported a vacuum assisted assembly of PS1 particles on gold electrodes which had been modified with SAMs bearing  $-NH_2$ ,  $-COOH$  and  $-CH_3$  terminal groups for electrostatic binding as well as N-hydroxysuccinimide (NHS) and terephthalaldehyde (TPDA) modified surfaces for covalent binding of PS1. Interestingly, the highest protein film thickness ( $72 \pm 9 \text{ \AA}$ )—achieved on bare gold electrodes—yielded the highest photocurrent densities approximately up to  $100 \text{ nA cm}^{-2}$ . In this case, the diffusing redox mediator 2,6-dichlorophenolindophenol

**Table 2** Summary: Photocurrents with PS1<sup>a</sup>

Procedure	Donor	Acceptor	Current density ( $\mu\text{A cm}^{-2} \text{mW}^{-1}$ )	Ref.
Bare gold	Na-ascorbate/DCPIP		0.01 <sup>b</sup>	60
TPDA-SAM on nanoporous gold	Na-ascorbate/DCPIP		0.4	62
Aminoethanethiol-SAM	$\text{K}_3[\text{Fe}(\text{CN})_6]/\text{K}_4[\text{Fe}(\text{CN})_6]$		0.15	63
NQC15S-AuNP on gold	Na-ascorbate/DCPIP	NQC15	0.007	59
NQC15EV on gold	Na-ascorbate/DCPIP	NQC15EV	0.12	67
3-mercapto-1-propanesulfonic acid SAM	DCPIP	MV	0.5	68
Bis-aniline-NP-Pt-Fd-NP/PS1 composite	Na-ascorbate/DCPIP	Bis-aniline-NP; Fd	1.38	72
Os complex modified polymer	Os complexes/MV	MV	17	75

<sup>a</sup> All current densities were standardised to an irradiation intensity of  $1 \text{ mW cm}^{-2}$ . <sup>b</sup> Irradiation intensity not reported.

(DCPIP) in combination with sodium ascorbate as electron donor provided the electrical contact between PS1 and the electrode. As DCPIP could simultaneously act as electron donor and acceptor, which would result in a zero net current, it is likely that ascorbate acts as a sacrificial reagent which reduces DCPIP in a homogeneous reaction in solution shifting the equilibrium towards  $\text{DCPIP}_2$ . Due to the low redox potential of the terminal iron-sulfur cluster  $F_B$  ( $E_0(F_B/F_B^-) = -0.58 \text{ V}$ ) the reduction of  $\text{O}_2$  may contribute to the photocurrent generation.<sup>61</sup> The same set-up was used to immobilise PS1 on nanoporous gold leaf electrodes.<sup>62</sup> Due to the substantially increased surface area of this material improved photocurrent densities of up to  $0.4 \mu\text{A cm}^{-2} \text{mW}^{-1}$  could be achieved. Alternatively, a “dip and dry” method was applied to generate densely packed PS1 films on gold electrode surfaces:<sup>63,64</sup> in this case, a peak-shaped current response indicated mass transport limitations between PS1 and the electrode due to the high protein film density. The considerable increase in photocurrent response may be mainly due to the higher light intensity used in this study ( $95 \text{ mW cm}^{-2}$ , white light vs.  $0.5 \text{ mW cm}^{-2}$ , red light).<sup>62</sup> After normalisation photocurrent densities of about  $0.15 \mu\text{A cm}^{-2} \text{mW}^{-1}$  remain.

**b) Molecular wires.** The intrinsic ET chain of PS1 can especially be modified or “engineered” at the acceptor side—an advantage which was realized by “wiring” PS1 to a gold electrode with a surface bound naphthoquinone-derivate (NQ).<sup>59</sup> A prerequisite for this is the fact that the  $A_1$ -cofactor of PS1—a phyloquinone—can be extracted from the protein environment with organic solvents such as diethyl ether or hexane.<sup>65,66</sup> The vacant  $A_1$ -site can then be reconstituted with a phyloquinone analogue such as NQ (1-[15-(3-methyl-1,4-naphthoquinon)]pentadecyl thiol) which is simultaneously bound to a gold nanoparticle (NP). By this, the protein bound gold NP can be further used for the immobilisation of the modified PS1 at a gold electrode surface *via* a bridging dithiol moiety (1,4-benzenedimethanethiol; Fig. 7).

It is assumed that the PS1 is orientated towards the electrode surface, thus facilitating direct ET communication at the formal potential of the  $A_1$  site ( $E_0(A_1/A_1^-) = -0.8 \text{ V}$ ). The reconstitution of PS1 with the NQ/gold NP was convincingly shown by TEM imaging. The surface coverage of the immobilised PS1 was determined to be  $0.7 \text{ pMol cm}^{-2}$ , which is a reasonable number assuming monolayer coverage. Although the photocurrent of  $7 \text{ nA cm}^{-2} \text{mW}^{-1}$  obtained in presence of DCPIP/ascorbate as

electron donor was rather poor, the immobilisation of this construct onto a thin  $\text{Si}_3\text{N}_4$ - $\text{Ta}_2\text{O}_5$  layer of the gate of a field effect transistor using silane coupling chemistry demonstrated the application of PS1 as a bio-photosensor in an imaging device.

In another study, a viologen-derivate (NQC15EV) was placed at the end of the molecular wire as electron relay instead of the gold NP.<sup>67</sup> In this case, electrons from the  $A_1$ -site were directly transferred to the electrode, which considerably improved the photocurrent to up to  $120 \text{ nA cm}^{-2} \text{mW}^{-1}$ . However, as compared with the theoretical value, the photocurrent is still small. Possibly, the molecular wire is not sufficiently conducting due to the lack of a conjugated  $\pi$ -electron system and thus cannot provide a fast ET rate. The observed photocurrent represents the net current: as mentioned above, oxidation of the acceptor (NQ15-viologen) and reduction of the donor (DCPIP) occur simultaneously due the external bias ( $0 \text{ V vs. Ag/AgCl}$ ) applied to the electrode. Therefore, the ET efficiency of the reaction occurring *via* the molecular wire itself

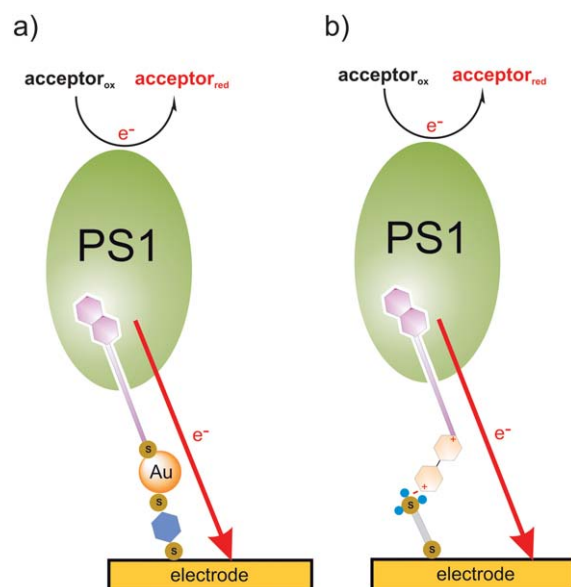


**Fig. 7** Concept of a PS1-based “bio-photosensor” in which PS1 is coupled with a gold electrode surface *via* a molecular wire. a) PS1 is attached to a gold surface *via* a composite of 1,4-benzodithiol-Au-NP-NQC15S. b) Attachment *via* a 1,4-benzodithiol-viologen-NQC15-composite (according to ref. 59, 67).

cannot be determined directly. Indirectly, the integrity of the wire was shown by time resolved absorption spectroscopy with absorbance changes of the viologen in the range of 20 ps reflecting the light induced reduction by  $A_0$ .<sup>67</sup>

Both studies represent good examples for acceptor-site wired PS1 on electrodes. If further optimized, this could be a strategy to utilize the power of light-driven charge separation at an early stage of the intrinsic ET. On the one hand this guarantees a high reducing power, and on the other hand the intrinsic ET reaction sequence is minimized. A considerable drawback for a practical large-scale application is, however, the time-consuming PS1 preparation and pretreatment. In an extension of this study, an improved and simplified procedure was presented which also showed improved photocurrent values.<sup>68</sup> To a gold surface, which was modified with a SAM of 3-mercaptopropylsulfonic acid, PS1 was bound by electrostatic interactions. In contrast to the work by Faulkner and Ciesielski,<sup>60,62-64</sup> methyl viologen ( $MV^{2+}$ ) was used as acceptor and DCPIP as electron donor. The reduction of  $MV^{2+}$  by the  $F_B^-$  side of PS1 follows the reaction scheme shown in Fig. 8.

As the reduction of  $O_2$  by  $MV^+$  is very fast ( $k = 10^8 \text{ M}^{-1} \text{ s}^{-1}$ ) and also about two orders of magnitude faster than the reduction of  $MV^{2+}$  by PS1 ( $k \sim 10^6 \text{ M}^{-1} \text{ s}^{-1}$ ),  $MV^+$  is hardly reoxidized at the electrode surface. Hence it should not notably effect the net photocurrent of up to  $\sim 0.5 \mu\text{A cm}^{-2} \text{ mW}^{-1}$ , which should only be governed by the diffusional mass transport of the redox mediators. Surprisingly, even under these conditions we are far away from the outstanding photon to charge conversion efficiency of PS1 in biological systems.

**c) Redox/conductive polymers.** Another possibility to wire PS1 to solid supports *via* components at its acceptor side is based on the capability of PS1 to photo-precipitate metal colloids like  $[\text{PtCl}_6]^{2-}$ ,  $[\text{OsCl}_6]^{2-}$  and  $[\text{IrCl}_6]^{2-}$ .<sup>69-71</sup>

In the presence of these nanoclusters which are electrically attached to the  $F_B$ -site, PS1 can produce  $H_2$  if an electron donor is available. This method was adapted successfully for the electropolymerisation of PS1 complexes onto electrode surfaces.<sup>72</sup> Pt

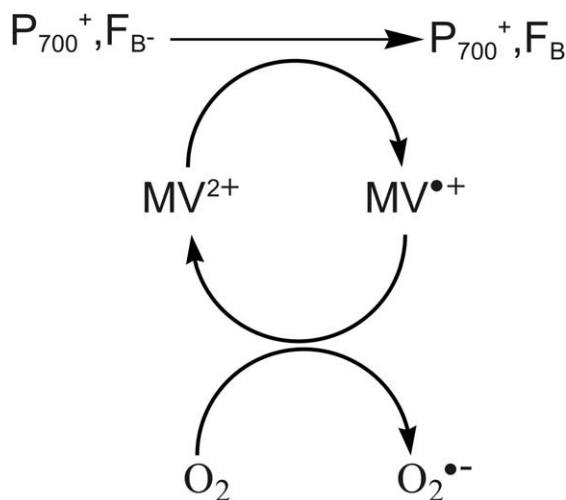


**Fig. 8** Reaction scheme of the acceptor site ( $F_B$ ) interaction of PS1 with methyl viologen.

nanoclusters associated with PS1 complexes were modified with thioaniline and further electropolymerized with thioaniline functionalized Pt- nanoparticles. The obtained bis-aniline-crosslinked PS1/Pt NP composite (see Fig. 9) was shown to participate in the ET from PS1 to the electrode depending on the electrode potential ( $>0 \text{ V vs. Ag/AgCl}$ ).

Typical photocurrent responses were in the range of  $1 \mu\text{A cm}^{-2} \text{ mW}^{-1}$  which is equivalent to a photon to carrier conversion efficiency (IPCE) of 0.35%. Incorporation of the native PS1 electron acceptor ferredoxin into the matrix of the bis-aniline-Pt/PS1 composite facilitated the ET resulting in an enhanced photocurrent of  $1.38 \mu\text{A cm}^{-2} \text{ mW}^{-1}$  (IPCE = 0.5%).

These studies demonstrate the big variety of possible procedures for the integration of PS1 into bioelectrochemical devices. Interestingly, nearly all publications use DCPIP as electron donor, which is far from being the best choice as compared with other free diffusing reductants of the donor site ( $P_{700}$ ) of PS1, *e.g.* phenazine-methosulfate or the native electron donor cytochrome  $c_6$ .<sup>73,74</sup> In order to optimize the ET communication with the electrode surface it is therefore mandatory to improve the interaction with the donor site of PS1. This was achieved in our own work by using osmium complex containing redox polymers as electron donors for PS1.<sup>75</sup> Similar compounds were previously used together with PS2 in bioelectrochemical systems.<sup>35</sup> The major advantage is seen in the fact that the redox polymers act simultaneously as immobilisation matrix and as polymeric ET mediator. They provide an efficient ET pathway *via* a sequence of self-exchange reactions between adjacent polymer-bound Os-complexes, which is mainly, with the exception of the necessary movement of the counter ions during the redox process, mass transport independent.

The photogenerated charge separated state  $[P_{700}^+, F_B^-]$  can be either reduced by  $\text{Os}^{2+}$  or oxidized by  $MV^{2+}$ , with the coupled  $O_2$ -reduction providing a fast regeneration of the  $MV^{2+}$ . This set-up

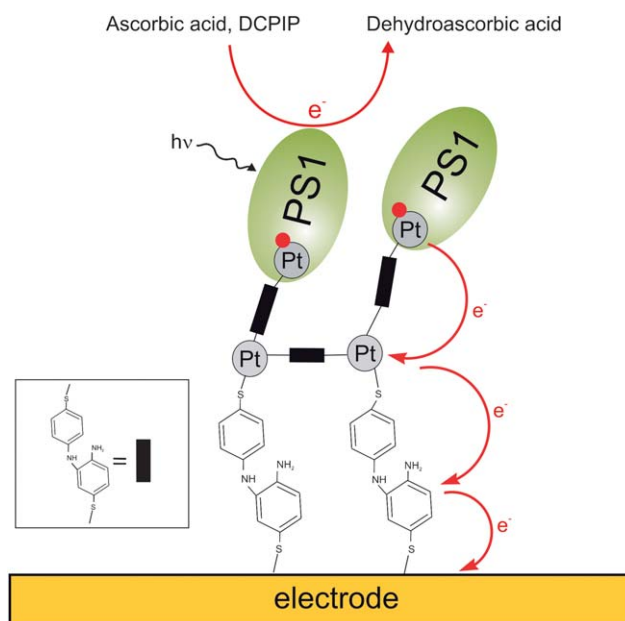


**Fig. 9** Schematic representation of a bis-aniline-crosslinked NP-Pt nanocluster/PS1 composite on an Au-electrode (according to ref. 72).



achieved average photocatalytic current responses of  $\sim 17 \mu\text{A cm}^{-2} \text{mW}^{-1}$  equivalent to an IPCE of 3.5%. The strong dependence of the photocurrent on the  $\text{O}_2$  concentration in solution indicated that the catalytic current is only limited by the mass transport of  $\text{MV}^{2+}$  or  $\text{O}_2$  and not by the donor-site interaction. Besides donor and acceptor sites, the generated photocurrents were also dependent on the light intensity and show a saturation curve, which reflects the rate limitation of the enzymatic catalysis. If treated according to Michaelis–Menten kinetics, determination of the kinetic parameters  $K_{\text{M/app}}$  ( $1.27 \text{ mW cm}^{-2}$  at 675 nm) and  $I_{\text{max/app}}$  ( $38 \mu\text{A cm}^{-2}$ ) was possible which can be advantageously used for comparison of different systems. Considering the fact that nearly all reports on bioelectrochemistry of PS1 are based on completely different light intensities and/or light quality, the need for standardization is more than obvious.

While the presented studies indicate how donor-site rate limitations could be overcome, the PS1 acceptor site is considered to be the real bottleneck for harvesting light energy. The only promising strategy to fully harvest the photocatalytic potential of PS1 may be the direct coupling of redox components at the acceptor site to desired reaction pathways.

### Application of wired photosystems: Towards photobiological production of hydrogen from water

One benefit of wired photosystems could be their use in engineered systems for photobiological hydrogen production.

In the broadest sense biological hydrogen production can be realized by three mutually supporting strategies:

- *Biological approach*: Microalgae (green algae or cyanobacteria) are “designed” via genetic modification for photobiological hydrogen production<sup>4,52</sup>

- *Artificial approach*: Bio-mimetic water-splitting systems are combined with hydrogen evolving catalysts<sup>76–79</sup>

- *Semi-artificial approach*: Isolated biological components are integrated into (photo)electrochemical devices.<sup>52,80,81</sup>

The latter strategy is within the scope of this article and fills the gap between artificial and biological approaches. In terms of efficiency, this approach is a benchmark for the development of either fully synthetic catalysts or self-reproducing biological “design” cells. Acting in series, PS1 and PS2 are particularly suitable as electron source for the reduction of protons, especially as their substrates are finally only water and visible light.

Due to its formal potential at the  $\text{F}_\text{B}$ -site ( $E^\circ = -580 \text{ mV vs. SHE}^1$ ), PS1 has the unique capability to produce  $\text{H}_2$ , since the driving force—considering the  $\text{H}^+$  reduction potential under physiological conditions ( $\text{pH} = 7$ ,  $\rho\text{H}_2 < 1 \mu\text{bar}$ ) of about  $-250 \text{ mV vs. SHE}$ —is very high.<sup>82</sup> However, as PS1 is not capable of reducing protons at the  $\text{Fe-S}$  cluster, a proton reducing catalyst has to be electrically connected to the acceptor site of PS1.

As mentioned above, the formation of nanoclusters from photoprecipitated metal colloids like  $[\text{PtCl}_6]^{2-}$  and the association with the  $\text{F}_\text{B}$ -site of PS1 can be utilized for the production of  $\text{H}_2$  with PS1.<sup>70,71</sup> This approach yielded  $\text{H}_2$ -rates of up to  $\sim 0.08 \mu\text{mol H}_2 (\text{mg Chl})^{-1} \text{h}^{-1}$ , obtained with isolated and platinized PS1 particles from spinach. Using this strategy, a considerable improvement with  $\text{H}_2$ -rates of up to  $5.5 \mu\text{mol H}_2 (\text{mg Chl})^{-1} \text{h}^{-1}$  was achieved with PS1 particles from the thermophilic

cyanobacterium *T. elongatus*.<sup>5</sup> Although the efficiency of this approach is still rather low as compared with the activity of isolated PS1-complexes—about  $1000 \mu\text{mol e}^- (\text{mg Chl})^{-1} \text{h}^{-1}$ —the simple preparation procedure is a major progress.<sup>6</sup>

A further improvement of the basic idea to link a metal catalyst to the acceptor site of PS1 was achieved by a PS1-mutant (C13G/C33S) from *Synechococcus* sp. PCC 7002 lacking a cysteine.<sup>83</sup> After assembly of the  $\text{Fe-S}$ -cluster in solution and reconstitution into an apo-PsaC-subunit, active PS1 complexes could be obtained. Instead of the missing cysteine, 1,6-hexanedithiol was used as covalent linker between  $\text{F}_\text{B}$  and a Pt-NP which catalysed proton reduction. This bioconjugate was capable of reducing protons with rates of  $\sim 50 \mu\text{mol H}_2 (\text{mg Chl})^{-1} \text{h}^{-1}$ . A further significant improvement with rates of  $>300 \mu\text{mol H}_2 (\text{mg Chl})^{-1} \text{h}^{-1}$  was obtained after crosslinking plastocyanin at the donor site and using 1,4-benzenedithiol as molecular wire between  $\text{F}_\text{B}$  and the Pt-NP.<sup>84</sup>

The amount of precious metals which are required for the production of hydrogen is limited on earth. They may be replaced by transition metals like Fe and Ni, which also form the active centers of hydrogenases and catalyse both the reduction of protons and the oxidation of  $\text{H}_2$ . These enzymes have been characterized in various electrochemical studies (for reviews see ref. 82 and 85). As revealed by protein film voltammetry,  $[\text{Ni-Fe}]$ -hydrogenases show a catalytic bias towards  $\text{H}_2$  oxidation and are at least as good as platinum.<sup>86</sup> In contrast,  $[\text{Fe-Fe}]$ -hydrogenases show much higher  $\text{H}_2$ -production activities<sup>87,88</sup> and are supposed to be an even better catalysts than platinum.<sup>89</sup> The disadvantage of both enzymes is their pronounced oxygen sensitivity, which in the case of  $[\text{Fe-Fe}]$ -hydrogenases leads to complete inactivation, whereas  $[\text{Ni-Fe}]$ -hydrogenases are reversibly inhibited and in very few cases even  $\text{O}_2$ -tolerant.<sup>87,88,90</sup>

Lubner *et al.*<sup>91</sup> reported the successful connection of PS1 and a  $[\text{Fe-Fe}]$ -hydrogenase from *Clostridium acetobutylicum* via a molecular wire, which was based on the principle used for the linkage of a Pt-NP (see above). A cysteine in the distal located  $[\text{4Fe-4S}]$  cluster of the hydrogenase was altered to glycine by site-directed mutagenesis resulting in a lacking coordination site for Fe. A covalent linkage between PS1 and the  $\text{H}_2$ ase was generated by 1,6-hexanedithiol. This construct achieved an activity of about  $30 \mu\text{mol H}_2 (\text{mg Chl})^{-1} \text{h}^{-1}$  which was lower than with PS1 linked to the Pt-particle.

Up to now, there is only one report on the integration of a PS1- $\text{H}_2$ ase construct in an electrochemical device.<sup>92</sup> In this case the membrane bound  $[\text{Ni-Fe}]$ - $\text{H}_2$ ase (MBH) from *Ralstonia eutropha* was genetically fused with the extrinsic PsaE-subunit of PS1.<sup>93</sup> For the assembly of the MBH-PsaE onto the electrode, immobilised PS1 complexes lacking the PsaE-subunit served as template. The observation of a weak, but significant  $\text{H}_2$  production rate ( $120 \pm 30 \text{ pmol H}_2 \text{ s}^{-1} \text{ cm}^{-2}$ ) as triggered by light suggests that electrons provided at the acceptor site of PS1 ( $\text{F}_{\text{A/B}}$ ) can be directly utilised to reduce protons to molecular hydrogen by the  $\text{H}_2$ ase. Notably, the specific surface activity of the hybrid complex ( $75 \text{ mol H}_2 \text{ s}^{-1} \text{ mol}^{-1}$  hybrid complex) is similar to MBH directly immobilized on a pyrolytic graphite edge electrode in the absence of PS1 ( $70 \text{ mol H}_2 \text{ s}^{-1} \text{ mol}^{-1}$  hybrid complex) and also in accordance with data obtained from measurements in solution.<sup>93</sup>

In order to produce hydrogen in combination with photobiological water splitting, the key enzyme PS2 has to be linked to

PS1 which in turn is coupled to an appropriate catalyst. Since the coproduction of oxygen and hydrogen would—via the “Knallgas reaction”—inevitably lead to a light driven *futile cycle*, water oxidation and proton reduction reactions have to be spatially separated. Such an arrangement within a photoelectrochemical cell is schematically shown in Fig. 10: While the anodic half-cell reaction  $2\text{H}_2\text{O} \rightarrow \text{O}_2 + 4\text{H}^+ + 4\text{e}^-$  supplies electrons—driven by immobilised PS2—the cathodic half-cell reaction:  $4\text{H}^+ + 4\text{e}^- \rightarrow 2\text{H}_2$  is catalysed by PS1 in combination with an appropriate catalyst. Charge balance can be reached by separation of the half cells with a proton transfer membrane such as Nafion®.

In view of the reported recent progress, the realization of this kind of approach is within reach. If successful, it could serve as a blueprint for the further development of artificial as well as natural devices for hydrogen production. The advantage of such a photoelectrochemical cell is that each component can be individually characterized for its maximum potential and optimized to reach its maximum performance under defined conditions.

### Further considerations

Within the last decade, the bioelectrochemical investigation of electrodes modified with either PS1 or PS2 became an increasingly important field of research. On the one hand, this is due to the fact that the 3D structures of PS1 and PS2 have been solved up to the molecular level.<sup>9,94</sup> On the other hand, it is due to the outstanding catalytic performance of PS1 and PS2. Besides their important function as model compounds for energy related devices, their use as biosensors for environmental screening and optoelectronic devices are promising applications. Notably, as PS1 and PS2 have been optimized for billions of years for their function within living cells, under given thermodynamic constraints,<sup>95</sup> their adaptation for technological applications causes problems especially due to the instability of the isolated enzymes. In the cellular environment, they are maintained by repair and biogenesis cycles<sup>41,42</sup> which cannot be realized in a semi-artificial set-up. However, there are good examples, for nearly non-invasive modifications, such as the introduction of “molecular wires” which direct the catalysis towards the desired reactions. The design of appropriate ET pathways has to go beyond the synthesis of suitable redox components by including also protein engineering. Especially in case of PS2, which is known to be sensitive for damage by light, the combination of both strategies—an optimized ET and a stabilized protein

structure—could finally lead to a higher long-term stability and a more “robust” performance.<sup>96</sup> In the case of PS1 further progress could lead to minimal protein complexes which are completely adapted to perform the envisaged chemical reactions.

Besides applications, another important aspect of bioelectrochemical devices gaining a better understanding of the intrinsic ET reactions in PS2 and PS1, which could be important blueprints for the development of completely artificial photosystems. In contrast to small enzymes like  $\text{H}_2$ ases, which can easily be adsorbed on carbon surfaces for performing direct electrochemistry, photosynthetic proteins are impaired for such measurements by their large size. This can be overcome by molecular wires as well as by any kind of specifically designed redox mediators.

### Acknowledgements

We are grateful to A. Trebst for stimulating discussions and critical reading of the manuscript. Support by the Federal Ministry of Education and Research (BMBF, project  $\text{H}_2$  design cells) and the EU/NEST project “Solar- $\text{H}_2$ ” is also gratefully acknowledged.

### References

- 1 K. Brettel and W. Leibl, *Biochim. Biophys. Acta, Bioenerg.*, 2001, **1507**, 100–114.
- 2 M. Grabolle and H. Dau, *Biochim. Biophys. Acta, Bioenerg.*, 2005, **1708**, 209–218.
- 3 H. Bottin and B. Lagoutte, *Biochim. Biophys. Acta, Bioenerg.*, 1992, **1101**, 48–56.
- 4 B. Esper, A. Badura and M. Rögner, *Trends Plant Sci.*, 2006, **11**, 543–549.
- 5 I. J. Iwuchukwu, M. Vaughn, N. Myers, H. O’Neill, P. Frymier and B. D. Bruce, *Nat. Nanotechnol.*, 2009, **5**, 73–79.
- 6 E. El-Mohsnawy, M. J. Kopcak, E. Schlodder, M. Nowaczyk, H. E. Meyer, B. Warscheid, N. V. Karapetyan and M. Rögner, *Biochemistry*, 2010, **49**, 4740–4751.
- 7 H. Kuhl, J. Kruij, A. Seidler, A. Krieger-Liszakay, M. Bunker, D. Bald, A. J. Scheidig and M. Rögner, *J. Biol. Chem.*, 2000, **275**, 20652–20659.
- 8 K. N. Ferreira, T. M. Iverson, K. Maghlaoui, J. Barber and S. Iwata, *Science*, 2004, **303**, 1831–1838.
- 9 A. Guskov, J. Kern, A. Gabdulkhakov, M. Broser, A. Zouni and W. Saenger, *Nat. Struct. Mol. Biol.*, 2009, **16**, 334–342.
- 10 P. Jordan, P. Fromme, H. T. Witt, O. Klukas, W. Saenger and N. Krauss, *Nature*, 2001, **411**, 909–917.
- 11 Y. Umena, K. Kawakami, J. R. Shen and N. Kamiya, *Nature*, 2011, **473**, 55–60.
- 12 K. Habermüller, M. Mosbach and W. Schuhmann, *Fresenius J. Anal. Chem.*, 2000, **366**, 560–568.
- 13 I. Willner and E. Katz, *Angew. Chem., Int. Ed.*, 2000, **39**, 1180.
- 14 R. A. Marcus and N. Sutin, *Biochim. Biophys. Acta.*, 1985, **811**, 265–322.
- 15 G. Renger and T. Renger, *Photosynth. Res.*, 2008, **98**, 53–80.
- 16 Y. Miloslavina, M. Szczepaniak, M. G. Müller, J. Sander, M. Nowaczyk, M. Rögner and A. R. Holzwarth, *Biochemistry*, 2006, **45**, 2436–2442.
- 17 G. Raszewski and T. Renger, *J. Am. Chem. Soc.*, 2008, **130**, 4431–4446.
- 18 A. R. Holzwarth, M. G. Müller, M. Reus, M. Nowaczyk, J. Sander and M. Rögner, *Proc. Natl. Acad. Sci. U. S. A.*, 2006, **103**, 6895–6900.
- 19 G. Raszewski, B. A. Diner, E. Schlodder and T. Renger, *Biophys. J.*, 2008, **95**, 105–119.
- 20 J. Kern and G. Renger, *Photosynth. Res.*, 2007, **94**, 183–202.
- 21 K. Satoh, H. Koike, T. Ichimura and S. Katoh, *Biochim. Biophys. Acta, Bioenerg.*, 1992, **1102**, 45–52.
- 22 W. Oettmeier, S. Reimer and A. Trebst, *Plant Sci. Lett.*, 1974, **2**, 267–271.

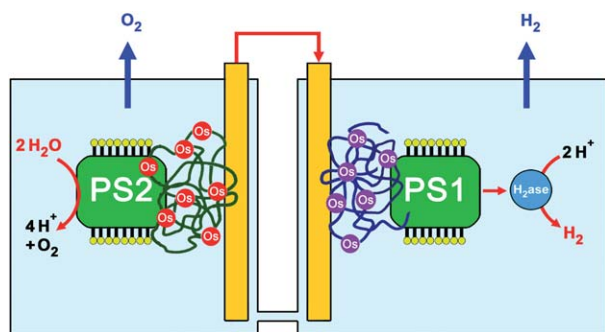


**Fig. 10** Proposed model for the photoelectrochemical production of hydrogen by PS2-based enzymatic water oxidation (according to ref. 30).

- 23 W. Oettmeier, *Cell. Mol. Life Sci.*, 1999, **55**, 1255–1277.
- 24 M. Koblížek, J. Maly, J. Masojídek, J. Komenda, T. Kučera, M. T. Giardi, A. K. Mattoo and R. Pilloton, *Biotechnol. Bioeng.*, 2002, **78**, 110–116.
- 25 J. Maly, J. Krejci, M. Ilie, L. Jakubka, J. Masojídek, R. Pilloton, K. Sameh, P. Steffan, Z. Stryhal and M. Sugiura, *Anal. Bioanal. Chem.*, 2005, **381**, 1558–1567.
- 26 M. T. Giardi and E. Pace, *Trends Biotechnol.*, 2005, **23**, 257–263.
- 27 K. Ataka, F. Giess, W. Knoll, R. Naumann, S. Haber-Pohlmeier, B. Richter and J. Heberle, *J. Am. Chem. Soc.*, 2004, **126**, 16199–16206.
- 28 G. B. Sigal, C. Bamdad, A. Barberis, J. Strominger and G. M. Whitesides, *Anal. Chem.*, 1996, **68**, 490–497.
- 29 J. Maly, J. Masojídek, A. Masci, M. Ilie, E. Cianci, V. Foglietti, W. Vastarella and R. Pilloton, *Biosens. Bioelectron.*, 2005, **21**, 923–932.
- 30 A. Badura, B. Esper, K. Ataka, C. Grunwald, C. Woll, J. Kuhlmann, J. Heberle and M. Rögner, *Photochem. Photobiol.*, 2006, **82**, 1385–1390.
- 31 K. Habermüller, A. Ramanavicius, V. Laurinavicius and W. Schuhmann, *Electroanalysis*, 2000, **12**, 1383–1389.
- 32 Y. Ling, M. Haemmerle, A. J. J. Olsthoorn, W. Schuhmann, H. L. Schmidt, J. A. Duine and A. Heller, *Anal. Chem.*, 1993, **65**, 238–241.
- 33 T. J. Ohara, *Platinum Met. Rev.*, 1995, **39**, 54–62.
- 34 T. J. Ohara, R. Rajagopalan and A. Heller, *Anal. Chem.*, 1993, **65**, 3512–3517.
- 35 A. Badura, D. Guschin, B. Esper, T. Kothe, S. Neugebauer, W. Schuhmann and M. Rögner, *Electroanalysis*, 2008, **20**, 1043–1047.
- 36 M. Hakala, I. Tuominen, M. Keranen, T. Tyystjarvi and E. Tyystjarvi, *Biochim. Biophys. Acta, Bioenerg.*, 2005, **1706**, 68–80.
- 37 I. Vass, K. Cser and O. Cheregi, *Ann. N. Y. Acad. Sci.*, 2007, **1113**, 114–122.
- 38 D. Guschin, J. Castillo, N. Dimcheva and W. Schuhmann, *Anal. Bioanal. Chem.*, 2010, **398**, 1661–1673.
- 39 M. W. Kanan, Y. Surendranath and D. G. Nocera, *Chem. Soc. Rev.*, 2009, **38**, 109–114.
- 40 H. Dau and I. Zaharieva, *Acc. Chem. Res.*, 2009, **42**, 1861–1870.
- 41 M. M. Nowaczyk, R. Hebel, E. Schlodder, H. E. Meyer, B. Warscheid and M. Rögner, *Plant Cell*, 2006, **18**, 3121–3131.
- 42 E. M. Aro, M. Suorsa, A. Rokka, Y. Allahverdiyeva, V. Paakkarinen, A. Saleem, N. Battchikova and E. Rintamaki, *J. Exp. Bot.*, 2005, **56**, 347–356.
- 43 M. Edelman and A. Mattoo, *Photosynth. Res.*, 2008, **98**, 609.
- 44 M. Vittadello, M. Y. Gorbunov, D. T. Mastrogiovanni, L. S. Wielunski, E. L. Garfunkel, F. Guerrero, D. Kirilovsky, M. Sugiura, A. W. Rutherford, A. Safari and P. G. Falkowski, *ChemSusChem*, 2010, **3**, 471–475.
- 45 A. Aoki and A. Heller, *J. Phys. Chem.*, 1993, **97**, 11014–11019.
- 46 A. Nakamura, T. Suzawa, Y. Kato and T. Watanabe, *FEBS Lett.*, 2005, **579**, 2273–2276.
- 47 A. N. Webber and W. Lubitz, *Biochim. Biophys. Acta, Bioenerg.*, 2001, **1507**, 61–79.
- 48 A. R. Holzwarth, M. G. Müller, J. Niklas and W. Lubitz, *Biophys. J.*, 2006, **90**, 552–565.
- 49 M. G. Müller, J. Niklas, W. Lubitz and A. R. Holzwarth, *Biophys. J.*, 2003, **85**, 3899–3922.
- 50 M. G. Müller, C. Slavov, R. Luthra, K. E. Redding and A. R. Holzwarth, *Proc. Natl. Acad. Sci. U. S. A.*, 2010, **107**, 4123–4128.
- 51 L. Frolov, Y. Rosenwaks, C. Carmeli and I. Carmeli, *Adv. Mater.*, 2005, **17**, 2434–2437.
- 52 N. Waschewski, G. Bernát and M. Rögner, in *Biomass to Biofuels: Strategies for Global Industries*, ed. N. Q. A. Vertès, H. Blaschek and H. Yukawa, John Wiley & Sons, Ltd., 2010, pp. 387–401.
- 53 R. Das, P. J. Kiley, M. Segal, J. Norville, A. A. Yu, L. Wang, S. A. Trammell, L. E. Reddick, R. Kumar, F. Stellacci, N. Lebedev, J. Schnur, B. D. Bruce, S. Zhang and M. Baldo, *Nano Lett.*, 2004, **4**, 1079–1083.
- 54 I. Carmeli, L. Frolov, C. Carmeli and S. Richter, *J. Am. Chem. Soc.*, 2007, **129**, 12352.
- 55 K. Brettel, *Biochim. Biophys. Acta, Bioenerg.*, 1997, **1318**, 322–373.
- 56 I. Lee, J. W. Lee and E. Greenbaum, *Phys. Rev. Lett.*, 1997, **79**, 3294–3297.
- 57 B. Munge, S. K. Das, R. Ilagan, Z. Pendon, J. Yang, H. A. Frank and J. F. Rusling, *J. Am. Chem. Soc.*, 2003, **125**, 12457–12463.
- 58 M. Ciobanu, H. A. Kincaid, V. Lo, A. D. Dukes, G. Kane Jennings and D. E. Cliffel, *J. Electroanal. Chem.*, 2007, **599**, 72–78.
- 59 N. Terasaki, N. Yamamoto, K. Tamada, M. Hattori, T. Hiraga, A. Tohri, I. Sato, M. Iwai, M. Iwai, S. Taguchi, I. Enami, Y. Inoue, Y. Yamanoi, T. Yonezawa, K. Mizuno, M. Murata, H. Nishihara, S. Yoneyama, M. Minakata, T. Ohmori, M. Sakai and M. Fujii, *Biochim. Biophys. Acta, Bioenerg.*, 2007, **1767**, 653–659.
- 60 C. J. Faulkner, S. Lees, P. N. Ciesielski, D. E. Cliffel and G. K. Jennings, *Langmuir*, 2008, **24**, 8409–8412.
- 61 D. C. Goetze and R. Carpentier, *J. Photochem. Photobiol., B*, 1990, **8**, 17–26.
- 62 P. N. Ciesielski, A. M. Scott, C. J. Faulkner, B. J. Berron, D. E. Cliffel and G. K. Jennings, *ACS Nano*, 2008, **2**, 2465–2472.
- 63 P. N. Ciesielski, C. J. Faulkner, M. T. Irwin, J. M. Gregory, N. H. Tolk, D. E. Cliffel and G. K. Jennings, *Adv. Funct. Mater.*, 2010, **20**, 4048–4054.
- 64 P. N. Ciesielski, F. M. Hijazi, A. M. Scott, C. J. Faulkner, L. Beard, K. Emmett, S. J. Rosenthal, D. Cliffel and G. Kane Jennings, *Bioresour. Technol.*, 2010, **101**, 3047–3053.
- 65 S. Itoh, M. Iwaki and I. Ikegami, *Biochim. Biophys. Acta, Bioenerg.*, 2001, **1507**, 115–138.
- 66 J. Biggins, *Biochemistry*, 1990, **29**, 7259–7264.
- 67 N. Terasaki, N. Yamamoto, T. Hiraga, Y. Yamanoi, T. Yonezawa, H. Nishihara, T. Ohmori, M. Sakai, M. Fujii, A. Tohri, M. Iwai, Y. Inoue, S. Yoneyama, M. Minakata and I. Enami, *Angew. Chem., Int. Ed.*, 2009, **48**, 1585–1587.
- 68 N. Terasaki, N. Yamamoto, M. Hattori, N. Tanigaki, T. Hiraga, K. Ito, M. Konno, M. Iwai, Y. Inoue, S. Uno and K. Nakazato, *Langmuir*, 2009, **25**, 11969–11974.
- 69 E. Greenbaum, *Science*, 1985, **230**, 1373–1375.
- 70 J. W. Lee, C. V. Tevault, S. L. Blankinship, R. T. Collins and E. Greenbaum, *Energy Fuels*, 1994, **8**, 770–773.
- 71 J. F. Millsaps, B. D. Bruce, J. W. Lee and E. Greenbaum, *Photochem. Photobiol.*, 2001, **73**, 630–635.
- 72 O. Yehezkel, O. I. Wilner, R. Tel-Vered, D. Roizman-Sade, R. Nechushtai and I. Willner, *J. Phys. Chem. B*, 2010, **114**, 14383–14388.
- 73 K. N. Gourovskaya, M. D. Mamedov, I. R. Vassiliev, J. H. Golbeck and A. Y. Semenov, *FEBS Lett.*, 1997, **414**, 193–196.
- 74 V. Proux-Delrouyre, C. Demaille, W. Leibl, P. Stetif, H. Bottin and C. Bourdillon, *J. Am. Chem. Soc.*, 2003, **125**, 13686–13692.
- 75 A. Badura, D. Guschin, T. Kothe, M. J. Kopczak, W. Schuhmann and M. Rögner, *Energy Environ. Sci.*, 2011, DOI: 10.1039/C1EE01126J.
- 76 D. Gust, T. A. Moore and A. L. Moore, *Acc. Chem. Res.*, 2009, **42**, 1890.
- 77 C. W. Cady, R. H. Crabtree and G. W. Brudvig, *Coord. Chem. Rev.*, 2008, **252**, 444–455.
- 78 R. Lomoth, A. Magnuson, M. Sjödin, P. Huang, S. Styring and L. Hammarström, *Photosynth. Res.*, 2006, **87**, 25–40.
- 79 C. Herrero, B. Lassalle-Kaiser, W. Leibl, A. W. Rutherford and A. Aukauloo, *Coord. Chem. Rev.*, 2008, **252**, 456–468.
- 80 S. O. Wenk, D.-J. Qian, T. Wakayama, C. Nakamura, N. Zorin, M. Rögner and J. Miyake, *Int. J. Hydrogen Energy*, 2002, **27**, 1489–1493.
- 81 W. Haehnel and H. J. Hochheimer, *J. Electroanal. Chem.*, 1979, **104**, 563–574.
- 82 K. A. Vincent, A. Parkin and F. A. Armstrong, *Chem. Rev.*, 2007, **107**, 4366–4413.
- 83 R. A. Grimme, C. E. Lubner, D. A. Bryant and J. H. Golbeck, *J. Am. Chem. Soc.*, 2008, **130**, 6308–6309.
- 84 R. A. Grimme, C. E. Lubner and J. H. Golbeck, *Dalton Trans.*, 2009, 10106–10113.
- 85 E. Reisner, *Eur. J. Inorg. Chem.*, 2011, **2011**, 1005–1016.
- 86 A. K. Jones, E. Sillery, S. P. J. Albracht and F. A. Armstrong, *Chem. Commun.*, 2002, 866–867.
- 87 M. Frey, *ChemBioChem*, 2002, **3**, 153–160.

- 
- 88 K. A. Vincent, A. Parkin, O. Lenz, S. P. J. Albracht, J. C. Fontecilla-Camps, R. Cammack, B. r. Friedrich and F. A. Armstrong, *J. Am. Chem. Soc.*, 2005, **127**, 18179–18189.
- 89 M. Hambourger, M. Gervaldo, D. Svedruzic, P. W. King, D. Gust, M. Ghirardi, A. L. Moore and T. A. Moore, *J. Am. Chem. Soc.*, 2008, **130**, 2015–2022.
- 90 T. Buhrke, O. Lenz, N. Krauss and B. r. Friedrich, *J. Biol. Chem.*, 2005, **280**, 23791–23796.
- 91 C. E. Lubner, P. Knörzer, P. J. Silva, K. A. Vincent, T. Happe, D. A. Bryant and J. H. Golbeck, *Biochemistry*, 2010, **49**, 10264–10266.
- 92 H. Krassen, A. Schwarze, B. Friedrich, K. Ataka, O. Lenz and J. Heberle, *ACS Nano*, 2009, **3**, 4055–4061.
- 93 M. Ihara, H. Nishihara, K. S. Yoon, O. Lenz, B. Friedrich, H. Nakamoto, K. Kojima, D. Honma, T. Kamachi and I. Okura, *Photochem. Photobiol.*, 2006, **82**, 676–682.
- 94 I. Grotjohann and P. Fromme, *Photosynth. Res.*, 2005, **85**, 51–72.
- 95 J. W. Schopf, *Photosynth. Res.*, 2011, **107**, 87–101.
- 96 O. Shlyk-Kerner, I. Samish, D. Kaftan, N. Holland, P. S. Maruthi Sai, H. Kless and A. Scherz, *Nature*, 2006, **442**, 827–830.